New insights into the reconstructed temperature in Portugal over the last 400-years

J. A. Santos[1], M. F. Carneiro[1], A. Correia[2], M. J. Alcoforado[3], E. Zorita[4], J. J. Gómez-Navarro[5]

[1] {Centre for the Research and Technology of Agro-Environmental and Biological Sciences, CITAB, Universidade de Trás-os-Montes e Alto Douro, UTAD, 5000-801 Vila Real, Portugal}

[2] {Department of Physics and Geophysical Centre of Évora, University of Évora, Évora, Portugal}

[3] {Centro de Estudos Geográficos, IGOT, Universidade de Lisboa, Ed. Faculdade de Letras, 1600-214 Lisboa, Portugal}

[4] {Institute for Coastal Research, Helmholtz-Zentrum Geesthacht, Geesthacht, Germany}

[5] {Climate and Environmental Physics, Physics Institute and Oeschger Centre for Climate Change Research, University of Bern, 3012 Bern, Switzerland}

Correspondence to: J. A. Santos (jsantos@utad.pt);

Abstract

The reliability of an existing reconstructed annual (December–November) temperature series for the Lisbon region (Portugal) from 1600 onwards, based on a European-wide reconstruction, is assessed in the present study. The consistency of this series with: (1) five local borehole temperature-depth profiles; (2) synthetic temperature-depth profiles generated from both reconstructed temperatures and two regional paleoclimate simulations in Portugal; (3) instrumental data sources over the twentieth century; and (4) temperature indices from documentary sources during the late Maunder Minimum (1675–1715) is assessed. It is found that the reconstructed annual mean temperature series in Portugal is not consistent with the external forcings from the regional paleoclimate simulations. Furthermore, the low-frequency variability in the simulations is in agreement with local borehole temperature-depth profiles. Therefore, the existing reconstructed series is calibrated by adjusting its low-frequency variability to the simulations (first-stage adjustment). The annual reconstructed series is then calibrated in its location and scale parameters, using the instrumental series and a linear regression between them (second-stage adjustment). This calibrated series shows clear footprints of the Maunder and Dalton minima, commonly related to changes in solar activity and explosive volcanic eruptions, and a strong recent-past warming, commonly related to human-driven forcing. Lastly, it is also in overall agreement with independently-derived annual temperature indices for the late Maunder Minimum. Thus, the series resulting from this post-reconstruction adjustment can be of foremost relevance to improve the current understanding of the driving mechanisms of climate variability in Portugal.

1. Introduction

Climate reconstructions allow further insight into the climatic variability beyond the relatively short instrumental period, being commonly based on early instrumental records, documentary evidence, namely memoirs, diaries, chronicles, weather logs, ship logbooks, and natural proxies, such as boreholes, tree-rings, corals, ice-cores, speleothem records, pollen-profiles (Brázdil et al., 2010; Brázdil et al., 2005; Camuffo et al., 2010; Li et al., 2010; Luterbacher et al., 2006; Pollack and Huang, 2000). Historical climatology is critical for understanding the driving processes of climate variability not only in the past, but also in the future. This is particularly important when developing climate change projections for the future under emission scenarios (IPCC, 2013).

Climate variability in Europe over the last millennium was reconstructed based on both documentary evidence and natural proxies (e.g. Alcoforado et al., 2000; Brázdil et al., 2010; Brázdil et al., 2005; Camuffo et al., 2013; González-Rouco et al., 2009; Luterbacher et al., 2006). European-wide temperature reconstructions since 1500 were already developed (Luterbacher et al., 2004; Xoplaki et al., 2005), as well as continental-wide reconstructions for the last two millennia by Ahmed et al. (2013). Temperature reconstructions in some European sites, based on both documentary data and instrumental records since the 16th century, were carried out by Camuffo et al. (2010). A temperature reconstruction for southern Portugal during the late Maunder Minimum (LMM; 1675-1715) was presented by Alcoforado et al. (2000). However, in Portugal, most of the pre-instrumental records show numerous temporal gaps and there is a substantial lack of natural proxies with clear climatic signals (Alcoforado et al., 2012; Camuffo et al., 2010; Luterbacher et al., 2006).

Borehole temperature-depth profiles can be used as paleoclimate proxies for climate reconstruction (e.g. Bodri and Čermák, 1997; González-Rouco et al., 2009; Majorowicz et al., 1999; Šafanda et al., 2007), as they provide independent information on long-term temperature variability (Jones et al., 2009). Borehole measurements are a complementary temperature record to high-frequency air temperature series recorded at weather stations and, through profile inversion methods, may also enable validating low-frequency variability in these series (e.g. Beltrami and Bourlon, 2004; Beltrami and Mareschal, 1995; Beltrami et al., 2011; Chouinard and Mareschal, 2007; González-Rouco et al., 2006; Gouirand et al., 2007; Harris and Chapman, 1998; Harris and Gosnold, 1999; Nielsen and Beck, 1989; Pollack et al., 2006). Some studies have been carried out using borehole temperature logs measured in southern Portugal (e.g.

75 Correia and Šafanda, 2001; Correia and Šafanda, 1999; Šafanda et al., 2007). Borehole
76 reconstructions can also be compared to paleoclimate simulations generated by Earth system
77 models for validation purposes (Beltrami et al., 2006; González-Rouco et al., 2009; Stevens et
78 al., 2008).

79 The present study aims at analysing the consistency between the Luterbacher et al. (2004) and
80 Xoplaki et al. (2005) temperature reconstructions for the Lisbon region (Portugal) and over the
81 period of 1600–1999 using: 1) five local borehole temperature-depth profiles; 2) synthetic
82 temperature-depth profiles, generated from gridded near-surface temperatures produced by
83 regional paleoclimate reconstructions and simulations; 3) instrumental data recorded in Lisbon
84 over the twentieth century; and 4) temperature indices from early instrumental and documentary
85 sources during the LMM (1675-1715). This analysis allows a validation of the annual mean
86 reconstructed temperature in Portugal over the last 400 years. The identification of possible
87 inconsistencies with the above-referred data sources enables a post-reconstruction adjustment
88 of this time series. In effect, this calibrated time series may help understanding past climate
89 variability in Portugal and its main driving mechanisms, namely the role of external vs. internal
90 forcing mechanisms on temperature variability. This attribution analysis provides critical
91 information for model validation and for assessing the reliability of regional climate change
92 projections. The datasets and methods are presented in section 2, the results are discussed in
93 section 3 and the main conclusions are summarized in section 4.

94

95 **2. Data and Methods**

96 **2.1 Reconstructed temperatures**

97 The reconstructed seasonal mean temperature in the gridbox (38.5–39.0˚N, 8.0–8.5˚W), which
98 is located in the area of Lisbon (Portugal), and for the period of 1600-1999 (Lut2004
99 henceforth) was extracted from the Luterbacher et al. (2004) and Xoplaki et al. (2005)
100 European-wide reconstructions. Data is originally defined on a 0.5˚ latitude × 0.5˚ longitude
101 grid. From 1901 onwards this dataset was based on instrumental data from New et al. (2000).
102 For the selected gridbox, it is largely based on temperature records from Lisbon. Since the
103 present study focuses on annual series, annual mean temperatures were obtained by averaging
104 the four values corresponding to winter (DJF), spring (MAM), summer (JJA) and autumn
105 (SON) mean temperatures (no monthly data is available). Hence, annual means refer to the

106   period from December of the previous year to November of that year (e.g. annual mean of 1710
107   corresponds to the average taken from December 1709 to November 1710).

108

2.2   Borehole data

110   The consistency of the Lut2004 reconstruction with borehole measurements retrieved from the
111   only geothermal-paleoclimatological observatory in Portugal (38.34° N; 7.58° W) is assessed.
112   It is located about 5 km northwestwards of Évora (southern Portugal) and about 100 km
113   eastwards of Lisbon. More detailed information about this observatory can be found in Correia
114   and Šafanda (2001) and Šafanda et al. (2007). Although the borehole measurements were not
115   taken in Lisbon, the variability in the 11-yr moving averages of annual mean temperatures in
116   Évora and Lisbon is quite similar (not shown). In fact, the correlation coefficient is of about
117   0.98 in their common instrumental period (1941-1999). The means for Lisbon and Évora are of
118   16.8ºC and 15.8ºC, respectively, while both standard deviations are of ca. 0.3ºC. Hence, these
119   borehole measurements are assumed to be representative of the measurements made in Lisbon,
120   as they mostly capture long-term variability.

121   Five measurements (temperature logs) in the same borehole TGQC1 are considered herein,
122   which were carried out on 24 March 1997 (M1), 27 March 2000 (M2), 14 November 2002
123   (M3), 26 November 2003 (M4), and 28 October 2004 (M5), respectively. These five
124   temperature logs were obtained by measuring the equilibrium temperature with a thermistor
125   every 5.0 m (M1), 1.0 m (M2), 2.5 m (M3 and M4) and 2.0 m (M5), along the ~190 m depth in
126   the borehole. The borehole is located in a region where the typical vegetation is old cork trees.
127   The vegetation type has not changed in the last hundred years and the topography is subdued,
128   with small elevation variations of tens of meters in the nearest few kilometres. The rock type in
129   the area is hercynian age granite. Its thermophysical properties were measured in four samples,
130   collected in a quarry located in the same granitic body and 1.5 km eastwards of the borehole.
131   Thermal conductivity values of 2.8 ± 0.2 W mK^{-1} and thermal diffusivity values of 1.3 ± 0.1
132   m^2 s^{-1} were measured on polished surfaces of rock samples. Heat production was calculated as
133   2 ± 1 W m^{-3} (Correia and Šafanda, 2001). The estimated heat flux density for the borehole is
134   60 mW m^{-2}, which was confirmed as an *a posteriori* value of 58 ± 13 mW m^{-2} using the
135   Functional Space Inversion method of Shen and Beck (1992).

136   The borehole temperature-depth profiles are herein compared to synthetic temperature profiles
137   (forward model), generated from both Lut2004 and annual mean near-surface temperatures

from paleoclimate simulations, rather than applying the conventional procedure of inverting temperature logs to reconstruct ground surface temperatures (e.g. Correia and Šafanda, 2001). However, the uncertainties inherent to these inversion models (Hartmann and Rath, 2005), mostly due to errors in the estimation of subsurface parameters, are also present in these forward models. The profiles were generated following the methodology described by Beltrami et al. (2011), as explained below.

The temperature anomaly at depth z and time t, due to a step change in surface temperature T_0, is given by the solution of the one-dimensional heat diffusion equation (Carslaw and Jaeger, 1959):

$$T(z,t) = T_0 erfc\left(\frac{z}{2\sqrt{kt}}\right),$$

(1)

where $erfc$ is the complementary error function and k is the subsurface thermal diffusivity (Cermak and Rybach, 1982). It has a value of 1.3×10^{-6} m^2s^{-1}, according to measurements on cut and polished surfaces of local rock samples (Correia and Šafanda, 2001). Generalizing this solution for a series of K step changes at the surface, the induced temperature anomalies at depth z are given by Mareschal and Beltrami (1992):

$$T_t(z) = T_i(z) + \sum_{j=1}^{K} T_j \left[erfc\left(\frac{z}{2\sqrt{kt_j}}\right) - erfc\left(\frac{z}{2\sqrt{kt_{j-1}}}\right) \right],$$

(2)

where $T_i(z)$ is the initial temperature profile.

2.3 Paleoclimate simulations

The paleoclimate simulations were carried out with the Global Circulation Model (GCM) – ECHO-G, and then dynamically downscaled with the Regional Climate Model (RCM) – MM5. ECHO-G combines the HOPE-G ocean model (Legutke and Voss, 1999) with the ECHAM4 atmospheric model (Roeckner et al., 1996). The regional model employs a limited area domain that spans completely the Iberian Peninsula with a spatial resolution of 30 km. Three reconstructed external forcings were used to consistently drive both models: solar variability, atmospheric greenhouse gas concentrations and radiative effects of stratospheric volcanic aerosols. The skill of the MM5/ECHO-G setup to reproduce the climate in the Iberian Peninsula has been previously evaluated by Gómez-Navarro et al. (2011), particularly with respect to the

166   ability of the regional model to reduce the warm bias and to correct the winter variability over
167   western Iberia in the GCM run. An ensemble of two paleoclimate simulations (Sim1 and Sim2),
168   only differing in their initial conditions, were used as a broad estimation of the effect of internal
169   variability (cf. Gómez-Navarro et al., 2012; González-Rouco et al., 2003; Zorita et al., 2007;
170   Zorita et al., 2005). Near-surface (2 m) temperatures for the period of 1600-1989 are extracted
171   from these simulations. Their daily mean fields were bilinearly interpolated from the original
172   MM5 grid to the reconstructed temperature grid ($0.5°$ latitude $\times 0.5°$ longitude) and extracted
173   for the above-defined Lisbon gridbox ($38.5–39.0°$N, $8.0–8.5°$W). Annual (December–
174   November) means were then computed from the raw 6-hourly data.

175   In order to identify low-frequency variability and trends in the paleoclimate simulations, a data-
176   adaptive filtering, based on a singular spectral analysis (SSA), is applied (Ghil and Vautard,
177   1991). SSA is based on the well-known principal component analysis, in which the multiple
178   dimensionality is achieved by including time-lagged replicas of the original time series. The
179   resulting principal components are thus linear combinations of different lags of this series,
180   which is equivalent to a time filtering with filter-coefficients that are related to the eigenvectors
181   of the lagged-covariance matrix. More formally, SSA corresponds to an eigenvalue
182   decomposition of a lagged-covariance matrix, with a Toeplitz structure, obtained from the
183   original time series of the paleoclimatic simulations. The rank, M, of this matrix is the average
184   of (N/4–N/3), where N is the time series length (Plaut and Vautard, 1994). For the paleoclimatic
185   simulations M=113 (N=390). In this methodology, the original time series can also be
186   decomposed into a sum of M additive components and can be partially rebuilt using only the
187   leading 'signal modes', thus filtering out background noisy components (Elsner and Tsonis,
188   1996; Vautard et al., 1992). In n-order SSA filtering, the leading n modes are used to rebuilt the
189   original time series. The lower the number of retained modes, the stronger is the time series
190   smoothing. If all M modes are used, the original time series is fully recovered.

191   Under the assumption that the aforementioned external forcings used in the paleoclimate
192   simulations are mainly manifested by long-term temperature trends in western Iberia, as
193   suggested by Gómez-Navarro et al. (2012), similar trends of reconstructed and simulated
194   temperatures should be expected. As SSA enables isolating data-adaptive non-linear trends in
195   the time series (Ghil and Vautard, 1991), it can be used to correct discrepancies between long-
196   term trends of reconstructed and simulated temperature series. In the present study, this
197   approach was used to adjust the low-frequency variability in the reconstructed series to the

7

198 paleoclimate external forcings obtained from the simulations (adjustment of the Lut2004
199 reconstruction). Therefore, instead of developing a new reconstruction, an adjustment of the
200 already existing reconstruction was carried out herein (post-reconstruction adjustment).

201

2.4 Instrumental data and indexed temperatures

203 The consistency of the Lut2004 reconstruction with the corresponding instrumental series
204 (InstT) for the available period of 1901–1999, recorded at the Lisboa-Geofísico meteorological
205 station and supplied by the European Climate Assessment & Dataset project (Klein Tank et al.,
206 2002), was also assessed. It should be stressed that Lut2004 is heavily dependent on InstT, as
207 previously referred, and a high temporal correspondence between these two time series is
208 thereby expected. A transfer-function between InstT and Lut2004 was determined by using a
209 linear regression analysis. The resulting first-order regression polynomial was applied so as to
210 calibrate the Lut2004 reconstruction in the extended period from 1600 onwards, thus correcting
211 its location and scale parameters. Lastly, annual indexed temperatures for southern Portugal
212 over the pre-instrumental period of 1675–1715 (LMM), developed by Alcoforado et al. (2000),
213 were also analysed for consistency assessment.

214

3. Results

3.1 Consistency with borehole measurements and paleoclimate simulations

217 The consistency of the Lut2004 reconstruction with borehole temperature-depth profiles and
218 with paleoclimate simulations is assessed in this section. The five logs of borehole
219 measurements (M1, M2, M3, M4 and M5) are shown in Fig. 1a. Their corresponding inverse
220 geothermal gradients were estimated using linear regressions applied to the bottom 140–180 m
221 data (Fig. 1b). Owing to the deposition of fine material at the bottom of the borehole, there is
222 locally a change in thermal conductivity at about 180 m. As the borehole was drilled in a very
223 homogeneous granite batholith, these changes are not due to changes in the geological
224 formation. In the present study, depths >180m are not used for gradient estimations. These
225 gradients approximately range from 46 to 48 m ºC^{-1} (ca. 0.021 ºC m^{-1}). The corresponding root-
226 mean squared error (RMSE) of each estimated linear model is always <0.01ºC (R-square
227 adjusted >99.9%), which means that the errors in the estimation of the geothermal gradients
228 have only minor impacts on the subsequent temperature-depth anomalies. The low borehole

229   depths require a word of caution, as some authors have indicated that 200 m of depth may be

230   too shallow for climate change assessments (Beltrami et al., 2011; Hamza et al., 2007;

231   Majorowicz et al., 1999). The Global Database of Borehole Temperatures and Climate

232   Reconstructions from University of Michigan and the World Data Center for Paleoclimatology

233   indeed consider a 200 m depth as a minimum requirement for past climate reconstruction

234   (Pollack and Huang, 2000). Beltrami et al. (2011) also demonstrated that the maximum depth

235   of borehole profiles can have a large impact on temperature-depth anomalies. Although no other

236   geothermal-paleoclimatological observatory is available in Portugal, the conclusions derived

237   from these borehole profiles may be provisional.

238   The five temperature-depth anomaly profiles (M1–5), after removing their estimated

239   geothermal gradients, are reproduced in Fig. 2a. M1, M2, M3 and M4 show a more pronounced

240   near-surface warming than M5. Overall, these profiles suggest strong recent-past warming

241   trends in near-surface air temperatures.

242   The synthetic temperature-depth anomaly profiles, generated from the Lut2004 reconstruction

243   and from the two paleoclimate simulations, are also shown in Fig. 2a. The 11–year running

244   means of their anomalies over the period 1600–1989 are plotted in Fig. 2b. The chronograms

245   of the two simulations, as well as their individual profiles, are indeed very similar to the

246   corresponding ensemble mean chronograms and profiles (not shown). In fact, the correlation

247   coefficient between the 11-yr running means of the two simulations is as high as +0.82. This is

248   indicative of the large influence of external forcings in the long-term variability of temperature.

249   Conversely to the simulations, which exhibit a strong warming trend since the 1830s, Lut2004

250   only depicts a recent-past upward trend and a cooling trend during the nineteenth century (Fig.

251   2b). Although the recent-past warming trend in Lut2004 is clearly corroborated by InstT, the

252   cooling trend is neither supported by simulations (Fig. 2b) nor by any scientific evidence from

253   previous studies. As a result, the synthetic temperature-depth anomaly profile obtained from

254   Lut2004 is remarkably different from the profiles obtained from the five borehole

255   measurements and from the paleoclimate simulations (Fig.2a).

256   The discussion above hints at a remarkable agreement between the low-frequency variability

257   of near-surface temperature from two independent sources (borehole measurements and

258   paleoclimate simulations). However, whereas the paleoclimate simulations agree well with the

259   borehole temperature-depth profiles, the reconstructed temperature for Portugal (Lut2004) fails

260   to capture the long-term trends. In fact, its linear trend is nearly zero over the whole period and

9

there is no signature of cool/warm periods. This striking disagreement between simulations and Lut2004 was already reported by Gómez-Navarro et al. (2011). As such, the low-frequency variability of the Lut2004 reconstruction needs to be adequately adjusted for climate research purposes. Towards this aim, the ensemble mean temperature from the two simulations was low-pass filtered by a 2-order SSA. The filtered series (SSA-trend in Fig. 2b) highlights the signature of the external forcings on near-surface temperature and was then added to the Lut2004 reconstruction. The resulting calibrated series (CalT = Lut2004 + SSA-trend) is also shown in Fig. 2b.

The SSA-trend clearly shows a warming trend since the 1830s and a relatively cool period during the LMM (1670–1730). This is also in line with previous studies on the impact of solar activity on global temperatures (e.g. Eddy, 1983; Frenzel, 1994). The period from 1730 to 1800 recorded annual mean temperatures close to the baseline, being followed by an anomalously cold period until the 1830s, which is associated with the Dalton Minimum, also a period of low solar activity (Wagner and Zorita, 2005). The strong upward trend in CalT from the 1830s onwards is now in clear agreement with the paleoclimate simulations and InstT (in the twentieth century). The LMM (ca. 1670–1730) and Dalton minimum (ca. 1790–1830) are also much clearer than in the Lut2004 reconstruction. Furthermore, the temperature-depth anomaly profile from CalT is similar to the profiles from the five borehole measurements and paleoclimate simulations (Fig. 2a). This represents an important validation of CalT.

3.2 Consistency with instrumental data

The consistency between InstT and CalT has been assessed by a linear regression in their common period (1901–1989). The corresponding scatterplot shows that linear regression provides a good fitting, with a correlation coefficient above 0.90 (Fig. 3), explaining about 82% of the total variance (R-square adjusted), and a RMSE of 0.22. According to the Fisher's test, this least-squares linear regression model is statistically significant at a 99% confidence level ($p<0.01$). A bootstrap procedure with 10,000 resamples shows that the 95% confidence interval for the correlation coefficient between InstT and CalT is [0.87, 0.93], supporting the Fisher's test. Therefore, CalT clearly reproduces the observed temperature in Portugal in the instrumental period (InstT). A 3-order polynomial fitting, with a robust regression using the bisquare weighting method, provides a slightly better adjustment (R-square adjusted of 83% and RMSE of 0.21), but its extrapolation for the lowest temperatures (outside the range of

293   values used in the model fitting, not shown) is not reliable and was discarded. The
294   corresponding linear regression polynomial is applied for a second-stage adjustment of location
295   and scale parameters in CalT. This allows expressing CalT in absolute temperature values
296   instead of anomalies (Fig. 4a). Additionally, taking into account the high coherency between
297   CalT and InstT, CalT was extended from 1989 to 1999 using InstT values. This final time series
298   can then be used, with high confidence, in upcoming studies of climate variability in Portugal.
299   The uncertainties in the CalT series are the combination of the original uncertainties in the
300   Lut2004 dataset plus additional uncertainties related to the non-linear trend used in the
301   adjustment. The former are discussed in detail in Luterbacher et al. (2004). The latter can be
302   estimated through the assessment of the consistence between Sim1 and Sim2. For this purpose,
303   the SSA filtering was applied separately to Sim1 and Sim2. The mean absolute difference
304   between the two non-linear trends obtained from Sim1 and Sim2 provides a measure of the
305   uncertainty related to the simulations. It has an approximate value of 0.05ºC. However, this
306   number provides just a lower bound, since it does not explicitly consider uncertainties related
307   to the simulation itself, which are difficult to assess due to the limited number of available
308   simulations with similar characteristics. In order to confirm long-term trends in CalT, the non-
309   parametric progressive Mann-Kendall test is applied (Sneyers, 1990, 1992). The forward and
310   backward Kendall t parameters for CalT jointly depict a warming trend from the 1830s
311   onwards, being particularly noteworthy since the 1930s (Fig.4b).

3.3 Consistency with precipitation indices

315   In previous studies, temperature in southern Portugal was analysed during the LMM (1675–
316   1715) by Alcoforado et al. (2000), and during the eighteenth century by Taborda et al. (2004)
317   and Alcoforado et al. (2012). In these studies, research was based on documentary evidence,
318   such as diaries, ecclesiastical rogation ceremonies (*pro-pluvia* and *pro-serenitate*),
319   *Misericórdias* and municipal institutional sources, as well as on early instrumental data. From
320   this documentary evidence, basic data were transformed into indices on an ordinal scale,
321   following the methodology developed by Pfister (1995). Monthly temperatures were originally
322   indexed on a scale from 0 to ±1. Annual indices (December–November) can then vary from 0
323   to ±12. The consistency between CalT and the corresponding annual indexed temperatures is
324   assessed by their respective scatterplots (Fig. 5). For a perfect agreement, the documented

temperature extremes (cold/hot years) should be reflected by coherent CalT anomalies, i.e. all data pairs in the scatterplots should be either on top-right or bottom-left quadrants (positively aligned series). There is an overall agreement between CalT and temperature indices (>80% of all years are on top-right or bottom-left quadrants, with a correlation coefficient of 0.76). Therefore, this agreement also provides a validation of CalT for the period of 1675–1715.

4. Summary and conclusions

The consistency of the reconstructed annual temperature series in Portugal (Lut2004) is assessed by using five borehole temperature-depth profiles, synthetic temperature-depth profiles, generated from both the Lut2004 reconstruction and paleoclimate simulations, instrumental data (InstT) and indexed temperatures during the LMM. While the paleoclimate simulations agree well with the borehole temperature-depth profiles, the same does not apply to the Lut2004 reconstruction. In fact, it fails to reproduce the long-term trend from the 1830s onwards. The late Maunder and Dalton minima, also clearly reflected in the paleoclimate simulations and well-documented in the literature, in association with changes in solar activity (Eddy, 1983), are both absent from the Lut2004 reconstruction. Moreover, there is a cooling trend throughout the nineteenth century that is not supported by previous studies. Therefore, the Lut2004 reconstruction was calibrated by adjusting its low-frequency variability to the paleoclimatic simulations, also in agreement with local borehole data. Documentary sources in Portugal during the LMM (1675–1715) also show high agreement with CalT, thus providing an additional validation over the LMM.

These results suggest some inability of the Lut2004 reconstruction to properly capture the low-frequency variability in Portugal. In effect, the absence of clear long-term trends in Lut2004 is not coherent with the significant changes in the radiative forcing throughout the last 400 years and the important role played by these external forcings on temperature variability over western Iberia (Gómez-Navarro et al., 2012). The frequent temporal gaps in the pre-instrumental records and the substantial lack of natural proxies with clear climatic signals in Portugal (Alcoforado et al., 2012; Camuffo et al., 2010; Luterbacher et al., 2006) may partially explain the inadequate reproduction of the low-frequency variability in the Lut2004 reconstruction. However, a severe loss of low-frequency variance caused by the method used in Lut2004 was also found by von Storch et al. (2009). Nevertheless, a more detailed assessment of the causes for this shortcoming

356 is out of the scope of the present study, as it does not develop a new reconstruction for
357 comparison, but rather an adjustment of an existing reconstruction.

358 Hence, CalT improves the Lut2004 reconstruction and can thus be of foremost relevance in
359 forthcoming research on climatic variability in Portugal. Due to the relatively coarse spatial
360 resolution of data generated by state-of-the-art GCMs, they are not suitable for regional-scale
361 assessments. Since such scales are precisely the focus of this study, temperature series from
362 two high-resolution regional paleoclimatic simulations (Sim1 and Sim2) are employed instead
363 of GCM runs. These two simulations were documented and validated in previous studies.
364 Unfortunately, there are only two available simulations covering Portugal with such high-
365 resolution characteristics. Hence, it is not possible to increase the ensemble size of model
366 simulations, though it would be very useful for uncertainty assessments. In forthcoming
367 research, new regional paleoclimatic simulations over Portugal, also using different models,
368 should be used to enhance the robustness and evaluate the significance of the current
369 adjustment.

370

376

References

377 Ahmed, M., Anchukaitis, K. J., Asrat, A., Borgaonkar, H. P., Braida, M., Buckley, B. M.,
378 Buntgen, U., Chase, B. M., Christie, D. A., Cook, E. R., Curran, M. A. J., Diaz, H. F., Esper,
379 J., Fan, Z. X., Gaire, N. P., Ge, Q. S., Gergis, J., Gonzalez-Rouco, J. F., Goosse, H., Grab, S.
380 W., Graham, N., Graham, R., Grosjean, M., Hanhijarvi, S. T., Kaufman, D. S., Kiefer, T.,
381 Kimura, K., Korhola, A. A., Krusic, P. J., Lara, A., Lezine, A. M., Ljungqvist, F. C., Lorrey,
382 A. M., Luterbacher, J., Masson-Delmotte, V., McCarroll, D., McConnell, J. R., McKay, N. P.,
383 Morales, M. S., Moy, A. D., Mulvaney, R., Mundo, I. A., Nakatsuka, T., Nash, D. J., Neukom,
384 R., Nicholson, S. E., Oerter, H., Palmer, J. G., Phipps, S. J., Prieto, M. R., Rivera, A., Sano, M.,
385 Severi, M., Shanahan, T. M., Shao, X. M., Shi, F., Sigl, M., Smerdon, J. E., Solomina, O. N.,
386 Steig, E. J., Stenni, B., Thamban, M., Trouet, V., Turney, C. S. M., Umer, M., van Ommen, T.,
387 Verschuren, D., Viau, A. E., Villalba, R., Vinther, B. M., von Gunten, L., Wagner, S., Wahl, E.
388 R., Wanner, H., Werner, J. P., White, J. W. C., Yasue, K., Zorita, E., and Consortium, P. k.:
389 Continental-scale temperature variability during the past two millennia, Nat. Geosci., 6, 339-
390 346, doi:10.1038/Ngeo1797, 2013.

392 Alcoforado, M. J., Nunes, M. F., Garcia, J. C., and Taborda, J. P.: Temperature and precipitation
393 reconstruction in southern Portugal during the late Maunder Minimum (AD 1675–1715),
394 Holocene, 10, 333–340, 2000.

395 Alcoforado, M. J., Vaquero, J. M., Trigo, R. M., and Taborda, J. P.: Early Portuguese
396 meteorological measurements (18th century), Clim. Past, 8, 353–371, doi:10.5194/cp-8-353-
397 2012, 2012.

398 Beltrami, H. and Bourlon, E.: Ground warming patterns in the Northern Hemisphere during the
399 last five centuries, Earth Planet. Sc. Lett., 227, 169–177, 2004.

400 Beltrami, H. and Mareschal, J.-C.: Resolution of ground temperature histories inverted from
401 borehole temperature data, Global Planet. Change, 11, 57–70, 1995.

402 Beltrami, H., González-Rouco, J. F., and Stevens, M. B.: Subsurface temperatures during the
403 last millennium: model and observation, Geophys. Res. Lett., 33, L09705,
404 doi:10.1029/2006GL026050, 2006.

405 Beltrami, H., Smerdon, J. E., Matharoo, G. S., and Nickerson, N.: Impact of maximum borehole
406 depths on inverted temperature histories in borehole paleoclimatology, Clim. Past, 7, 745–756,
407 doi:10.5194/cp-7-745-2011, 2011.

408 Bodri, L. and Čermák, V.: Reconstruction of remote climate changes from borehole
409 temperatures, Global Planet. Change, 15, 47-57, doi:10.1016/S0921-8181(97)00004-0, 1997.

410 Brázdil, R., Dobrovolný, P., Luterbacher, J., Moberg, A., Pfister, C., Wheeler, D., and Zorita,
411 E.: European climate of the past 500 years: new challenges for historical climatology, Climatic
412 Change, 101, 7-40, doi:10.1007/s10584-009-9783-z, 2010.

413 Brázdil, R., Pfister, C., Wanner, H., Storch, H., and Luterbacher, J.: Historical Climatology In
414 Europe – The State Of The Art, Climatic Change, 70, 363-430, doi:10.1007/s10584-005-5924-
415 1, 2005.

Camuffo, D., Bertolin, C., Barriendos, M., Dominguez-Castro, F., Cocheo, C., Enzi, S., Sghedoni, M., Valle, A., Garnier, E., Alcoforado, M. J., Xoplaki, E., Luterbacher, J., Diodato, N., Maugeri, M., Nunes, M. F., and Rodriguez, R.: 500-year temperature reconstruction in the Mediterranean Basin by means of documentary data and instrumental observations, Climatic Change, 101, 169-199, doi:10.1007/s10584-010-9815-8, 2010.

Camuffo, D., Bertolin, C., Diodato, N., Cocheo, C., Barriendos, M., Dominguez-Castro, F., Garnier, E., Alcoforado, M. J., and Nunes, M. F.: Western Mediterranean precipitation over the last 300 years from instrumental observations, Climatic Change, 117, 85-101, doi:10.1007/s10584-012-0539-9, 2013.

Carslaw, H. S. and Jaeger, J. C.: Conduction of Heat in Solids, Oxford Univ. Press, New York, 1959.

Cermak, V. and Rybach, L.: Thermal conductivity and specific heat of minerals and rocks. In: Subvolume A, Angenheister, G. (Ed.), Landolt-Börnstein - Group V Geophysics, Springer Berlin Heidelberg, 341–343, 1982.

Chouinard, C. and Mareschal, J. C.: Selection of borehole temperature depth profiles for regional climate reconstructions, Clim. Past, 3, 297-313, doi:10.5194/cp-3-297-2007, 2007.

Correia, A. and Šafanda, J.: Ground surface temperature history at a single site in southern Portugal reconstructed from borehole temperatures, Global Planet. Change, 29, 155-165, doi:10.1016/S0921-8181(01)00087-X, 2001.

Correia, A. and Šafanda, J.: Preliminary ground surface temperature history in mainland Portugal reconstructed from borehole temperature logs, Tectonophysics, 306, 269-275, doi:10.1016/S0040-1951(99)00060-8, 1999.

Eddy, J. A.: The Maunder Minimum - a Reappraisal, Sol. Phys., 89, 195-207, doi:10.1007/Bf00211962, 1983.

Elsner, J. B. and Tsonis, A. A.: Singular spectrum analysis: a new tool in time series analysis, Plenum Press, New York; London, 1996.

Frenzel, B.: Climatic Trends and anomalies in Europe 1675-1715. High resolution spatio-temporal reconstructions from direct meteorological observations and proxy data. Methods and Results, Gustav Fisher Verlag. Stuttgart, Jena and New York, 1994.

Ghil, M. and Vautard, R.: Interdecadal Oscillations and the Warming Trend in Global Temperature Time-Series, Nature, 350, 324-327, doi:10.1038/350324a0, 1991.

Gómez-Navarro, J. J., Montavez, J. P., Jerez, S., Jimenez-Guerrero, P., Lorente-Plazas, R., Gonzalez-Rouco, J. F., and Zorita, E.: A regional climate simulation over the Iberian Peninsula for the last millennium, Clim. Past, 7, 451-472, doi:10.5194/cp-7-451-2011, 2011.

Gómez-Navarro, J. J., Montávez, J. P., Jiménez-Guerrero, P., Jerez, S., Lorente-Plazas, R., González-Rouco, J. F., and Zorita, E.: Internal and external variability in regional simulations of the Iberian Peninsula climate over the last millennium, Clim. Past, 8, 25-36, doi:10.5194/cp-8-25-2012, 2012.

454 González-Rouco, F., von Storch, H., and Zorita, E.: Deep soil temperature as proxy for surface
455 air-temperature in a coupled model simulation of the last thousand years, Geophys. Res. Lett.,
456 30, 2116, doi:10.1029/2003GL018264, 2003.

457 González-Rouco, J. F., Beltrami, H., Zorita, E., and Stevens, M. B.: Borehole climatology: a
458 discussion based on contributions from climate modeling, Clim. Past, 5, 97-127,
459 doi:10.5194/cp-5-97-2009, 2009.

460 González-Rouco, J. F., Beltrami, H., Zorita, E., and von Storch, H.: Simulation and inversion
461 of borehole temperature profiles in surrogate climates: Spatial distribution and surface
462 coupling, Geophys. Res. Lett., 33, L01703, doi:10.1029/2005GL024693, 2006.

463 Gouirand, I., Moberg, A., and Zorita, E.: Climate variability in Scandinavia for the past
464 millennium simulated by an atmosphere-ocean general circulation model, Tellus A, 59, 30-49,
465 doi:10.1111/j.1600-0870.2006.00207.x, 2007.

466 Hamza, V. M., Cavalcanti, A. S. B., and Benyosef, L. C. C.: Surface thermal perturbations of
467 the recent past at low latitudes - inferences based on borehole temperature data from Eastern
468 Brazil, Clim. Past, 3, 513-526, 2007.

469 Harris, R. N. and Chapman, D. S.: Geothermics and climate change: 1. Analysis of borehole
470 temperatures with emphasis on resolving power, J. Geophys. Res.-Sol. Ea., 103, 7363-7370,
471 doi:10.1029/97JB03297, 1998.

472 Harris, R. N. and Gosnold, W. D.: Comparisons of borehole temperature–depth profiles and
473 surface air temperatures in the northern plains of the USA, Geophys. J. Int., 138, 541-548,
474 doi:10.1046/j.1365-246X.1999.00884.x, 1999.

475 Hartmann, A. and Rath, V.: Uncertainties and shortcomings of ground surface temperature
476 histories derived from inversion of temperature logs, J. Geophys. Eng., 2, 299,
477 doi:10.1088/1742-2132/2/4/S02, 2005.

478 IPCC: Climate Change 2013: The Physical Science Basis. Contribution of Working Group I to
479 the Fifth Assessment Report of the Intergovernmental Panel on Climate Change [Stocker, T.F.,
480 D. Qin, G.-K. Plattner, M. Tignor, S.K. Allen, J. Boschung, A. Nauels, Y. Xia, V. Bex and P.M.
481 Midgley (eds.)]. Cambridge University Press, Cambridge, United Kingdom and New York,
482 NY, USA, 1535 pp., 2013.

483 Jones, P. D., Briffa, K. R., Osborn, T. J., Lough, J. M., van Ommen, T. D., Vinther, B. M.,
484 Luterbacher, J., Wahl, E. R., Zwiers, F. W., Mann, M. E., Schmidt, G. A., Ammann, C. M.,
485 Buckley, B. M., Cobb, K. M., Esper, J., Goosse, H., Graham, N., Jansen, E., Kiefer, T., Kull,
486 C., Kuttel, M., Mosley-Thompson, E., Overpeck, J. T., Riedwyl, N., Schulz, M., Tudhope, A.
487 W., Villalba, R., Wanner, H., Wolff, E., and Xoplaki, E.: High-resolution palaeoclimatology of
488 the last millennium: a review of current status and future prospects, Holocene, 19, 3-49,
489 doi:10.1177/0959683608098952, 2009.

490 Klein Tank, A. M. G., Wijngaard, J. B., Können, G. P., Böhm, R., Demarée, G., Gocheva, A.,
491 Mileta, M., Pashiardis, S., Hejkrlik, L., Kern-Hansen, C., Heino, R., Bessemoulin, P., Müller-
492 Westermeier, G., Tzanakou, M., Szalai, S., Pálsdóttir, T., Fitzgerald, D., Rubin, S., Capaldo,
493 M., Maugeri, M., Leitass, A., Bukantis, A., Aberfeld, R., van Engelen, A. F. V., Forland, E.,
494 Mietus, M., Coelho, F., Mares, C., Razuvaev, V., Nieplova, E., Cegnar, T., Antonio López, J.,

495 Dahlström, B., Moberg, A., Kirchhofer, W., Ceylan, A., Pachaliuk, O., Alexander, L. V., and
496 Petrovic, P.: Daily dataset of 20th-century surface air temperature and precipitation series for
497 the European Climate Assessment, Int. J. Climatol., 22, 1441-1453, doi:10.1002/joc.773, 2002.

498 Legutke, S. and Voss, R.: The Hamburg atmosphere–ocean coupled circulation model ECHOG,
499 Germany DKRZ Tech. Rep. 18, Dtsch. Klimarechenzentrum, Hamburg, 1999.

500 Li, B., Nychka, D. W., and Ammann, C. M.: The Value of Multiproxy Reconstruction of Past
501 Climate, J. Am. Stat. Assoc., 105, 883-895, doi:10.1198/jasa.2010.ap09379, 2010.

502 Luterbacher, J., Dietrich, D., Xoplaki, E., Grosjean, M., and Wanner, H.: European seasonal
503 and annual temperature variability, trends, and extremes since 1500, Science, 303, 1499-1503,
504 doi:10.1126/science.1093877, 2004.

505 Luterbacher, J., Xoplaki, E., Casty, C., Wanner, H., Pauling, A., Küttel, M., Rutishauser, T.,
506 Brönnimann, S., Fischer, E., Fleitmann, D., Gonzalez-Rouco, F. J., García-Herrera, R.,
507 Barriendos, M., Rodrigo, F., Gonzalez-Hidalgo, J. C., Saz, M. A., Gimeno, L., Ribera, P.,
508 Brunet, M., Paeth, H., Rimbu, N., Felis, T., Jacobeit, J., Dünkeloh, A., Zorita, E., Guiot, J.,
509 Türkes, M., Alcoforado, M. J., Trigo, R., Wheeler, D., Tett, S., Mann, M. E., Touchan, R.,
510 Shindell, D. T., Silenzi, S., Montagna, P., Camuffo, D., Mariotti, A., Nanni, T., Brunetti, M.,
511 Maugeri, M., Zerefos, C., Zolt, S. D., Lionello, P., Nunes, M. F., Rath, V., Beltrami, H., Garnier,
512 E., and Ladurie, E. L. R.: Chapter 1 Mediterranean climate variability over the last centuries: A
513 review. In: Mediterranean climate variability, P. Lionello, Malanotte-Rizzoli, P., and Boscolo,
514 R. (Eds.), Elsevier, 2006.

515 Majorowicz, J. A., Šafanda, J., Harris, R. N., and Skinner, W. R.: Large ground surface
516 temperature changes of the last three centuries inferred from borehole temperatures in the
517 Southern Canadian Prairies, Saskatchewan, Global and Planet. Change, 20, 227-241,
518 doi:10.1016/S0921-8181(99)00016-8, 1999.

519 Mareschal, J. C. and Beltrami, H.: Evidence for recent warming from perturbed geothermal
520 gradients: examples from eastern Canada, Clim. Dynam., 6, 135-143,
521 doi:10.1007/BF00193525, 1992.

522 New, M., Hulme, M., and Jones, P.: Representing twentieth-century space-time climate
523 variability. Part II: Development of 1901-96 monthly grids of terrestrial surface climate, J.
524 Climate, 13, 2217-2238, 2000.

525 Nielsen, S. B. and Beck, A. E.: Heat-Flow Density Values and Paleoclimate Determined from
526 Stochastic Inversion of 4 Temperature Depth Profiles from the Superior Province of the
527 Canadian Shield, Tectonophysics, 164, 345-359, 1989.

528 Pfister, C.: Monthly temperature and precipitation in central Europe from 1525-1979:
529 quantifying documentary evidence on weather and its effects. In: Climate since A.D. 1500,
530 Bradley, R. S. and Jones, P. D. (Eds.), Routledge, London, 1995.

531 Plaut, G. and Vautard, R.: Spells of Low-Frequency Oscillations and Weather Regimes in the
532 Northern-Hemisphere, J. Atmos. Sci., 51, 210-236, 1994.

533 Pollack, H. N. and Huang, S. P.: Climate reconstruction from subsurface temperatures, Annu.
534 Rev. Earth. Pl. Sc., 28, 339-365, doi:10.1146/annurev.earth.28.1.339, 2000.

535   Pollack, H. N., Huang, S. P., and Smerdon, J. E.: Five centuries of climate change in Australia:
536   the view from underground, J. Quaternary Sci., 21, 701-706, doi:10.1002/Jqs.1060, 2006.

537   Roeckner, E., Arpe, K., Bengtsson, L., Christoph, M., Claussen, M., Dumenil, L., Esch, M.,
538   Giorgetta, M., Schlese, U., and Schulzweida, U.: The atmospheric general circulation model
539   ECHAM4: model description and simulation of present-day climate, Max-Planck-Institut für
540   Meterologie, Hamburg, Germany Tech. Rep., 218, 1996.

541   Šafanda, J., Rajver, D., Correia, A., and Dedecek, P.: Repeated temperature logs from Czech,
542   Slovenian and Portuguese borehole climate observatories, Clim. Past, 3, 453-462,
543   doi:10.5194/cp-3-453-2007, 2007.

544   Shen, P. Y. and Beck, A. E.: Paleoclimate Change and Heat-Flow Density Inferred from
545   Temperature Data in the Superior Province of the Canadian Shield, Global and Planetary
546   Change, 98, 143-165, 1992.

547   Sneyers, R.: On the Statistical Analysis of Series of Observations, Secretariat of the World
548   Meteorological Organization, Geneve, Switzerland, 1990.

549   Sneyers, R.: Use and measure of statistical methods for detection of climatic change, in: Climate
550   Change Detection Project. Report on the Informal Planning Meeting on Statistical Procedures
551   for Climate Change Detection, WCDMP, 20, 176–181, Geneve, Switzerland, 1992.

552   Stevens, M. B., González-Rouco, J. F., and Beltrami, H.: North American climate of the last
553   millennium: Underground temperatures and model comparison, J. Geophys. Res.-Earth, 113,
554   F01008, doi:10.1029/2006JF000705, 2008.

555   Taborda, J. P., Alcoforado, M. J., and Garcia, J. C.: Climate in southern Portugal in the 18th
556   century. Reconstruction based on documentary and early instrumental sources (in Portuguese,
557   with extended English summary), University of Lisbon, Geo-Ecologia, 2, CEG, Lisboa, ISBN:
558   972-636-144-3, 2004. http://clima.ul.pt/images/pdf/pub/b_mja_2004_climasulportugal.pdf

559   Vautard, R., Yiou, P., and Ghil, M.: Singular-Spectrum Analysis - a Toolkit for Short, Noisy
560   Chaotic Signals, Physica D, 58, 95-126, 1992.

561   von Storch, H., Zorita, E., and Gonzalez-Rouco, F.: Assessment of three temperature
562   reconstruction methods in the virtual reality of a climate simulation, Int. J. Earth Sci., 98, 67-
563   82, doi:10.1007/s00531-008-0349-5, 2009.

564   Wagner, S. and Zorita, E.: The influence of volcanic, solar and the Dalton Minimum (1790-
565   1830): CO2 forcing on the temperatures in a model study, Clim. Dyn., 25, 205-218,
566   doi:10.1007/s00382-005-0029-0, 2005.

567   Xoplaki, E., Luterbacher, J., Paeth, H., Dietrich, D., Steiner, N., Grosjean, M., and Wanner, H.:
568   European spring and autumn temperature variability and change of extremes over the last half
569   millennium, Geophys. Res. Lett., 32, L15713, doi:10.1029/2005GL023424, 2005.

570   Zorita, E., Gonzalez-Rouco, F., and von Storch, H.: Comments on "Testing the Fidelity of
571   Methods Used in Proxy-Based Reconstructions of Past Climate", J. Climate, 20, 3693-3698,
572   doi:10.1175/JCLI4171.1, 2007.

573   Zorita, E., González-Rouco, J. F., von Storch, H., Montávez, J. P., and Valero, F.: Natural and
574   anthropogenic modes of surface temperature variations in the last thousand years, Geophys.
575   Res. Lett., 32, L08707, doi:10.1029/2004GL021563, 2005.

576

Figure Captions

Fig. 1. (a) Borehole temperature logs (temperature vs. depth) for: M1, M2, M3, M4 and M5 from the Évora observatory (cf. legends). (b) The same as on (a), but only for the bottom 140–180 m data. The outlined equations of the respective regression lines (omitted) represent the corresponding estimated geothermal gradients (slope of the linear regression line).

Fig. 2. (a) Temperature-depth anomaly profiles for: M1, M2, M3, M4 and M5, with respect to the estimated geothermal gradients in Fig. 1b, along with the synthetic profiles generated from: Lut2004 – reconstructed temperature; CalT – calibrated temperature; and Sim1/Sim2 – paleoclimate simulations, retrieved for a gridbox near Lisbon, Portugal (cf. legends). (b) Chronograms of the 11-yr running mean anomalies of Lut2004, CalT and Sim1/Sim2 for the period of 1600–1989. The SSA filtered ensemble mean temperature from the two simulations (SSA-trend) is also displayed. The 11-yr running means of InstT (instrumental annual mean temperature) anomalies are depicted for the period of 1901-1999, along with the respective linear trend. Note that anomalies in each series are with respect to their common period (1901-1989).

Fig. 3. Scatterplot between InstT and CalT anomalies over their common period (1901–1989). The corresponding regression line, calibration equation and R-squared measure (determination coefficient) are also pointed out.

Fig. 4. Chronogram of: (a) CalT – calibrated annual mean temperature – in the period of 1600–1999 and InstT in the period of 1901–1999. Estimated errors are grey shaded, with a mean error of 0.05°C (b) Forward – u(t) – and backward – u'(t) – series of the normalised Kendall t parameter from the progressive Mann-Kendall analysis of CalT. 95% confidence interval for the no trend hypothesis in grey shading.

Fig. 5. Scatterplot of CalT in the period of 1675–1715 as a function of the annual temperature indices. Light (dark) grey circles represent cold (hot) years from documentary evidence. Circles with black edges indicate agreement between the two datasets. Years with '0' index are omitted for the sake of readability of the plot. The horizontal line corresponds to CalT mean. Some labels are omitted for the sake of clarity.
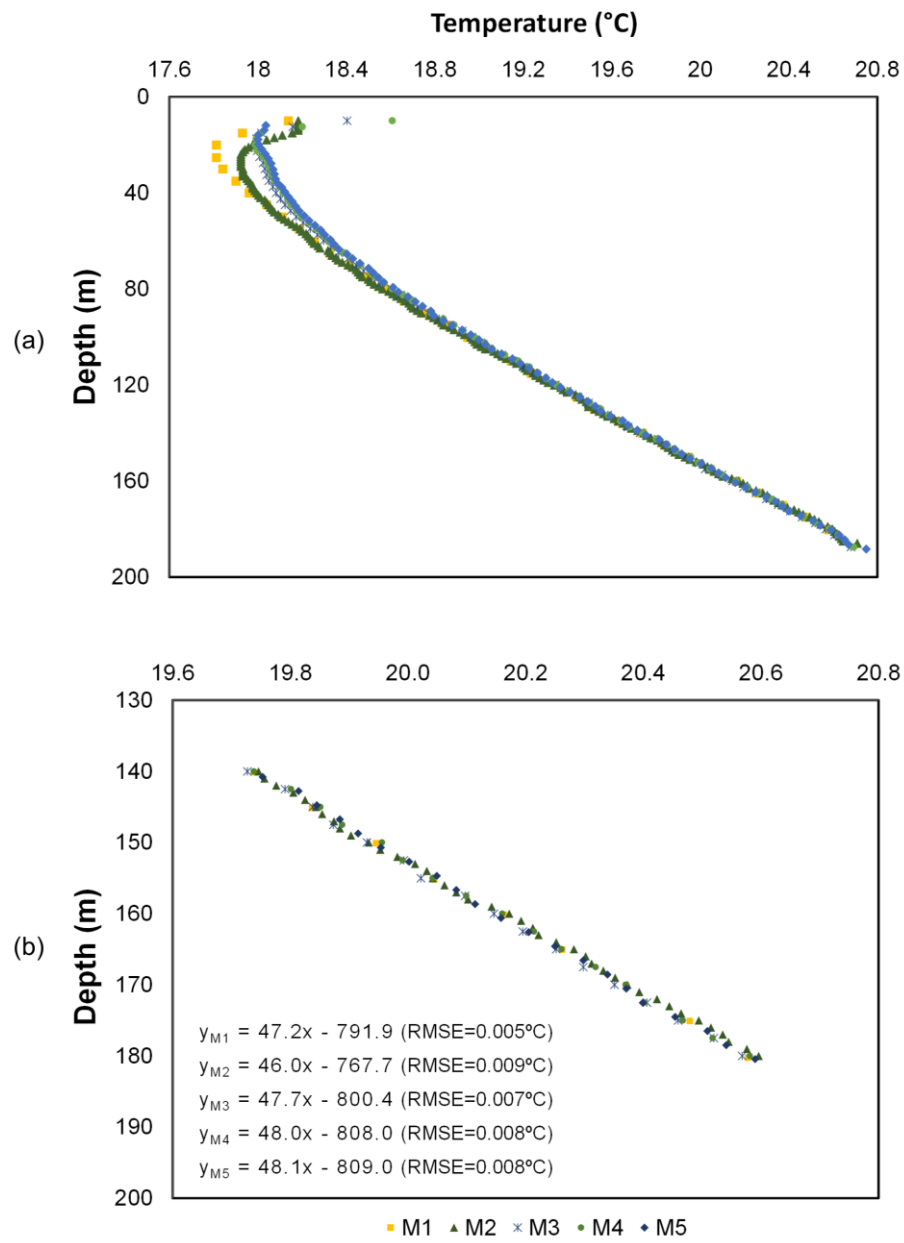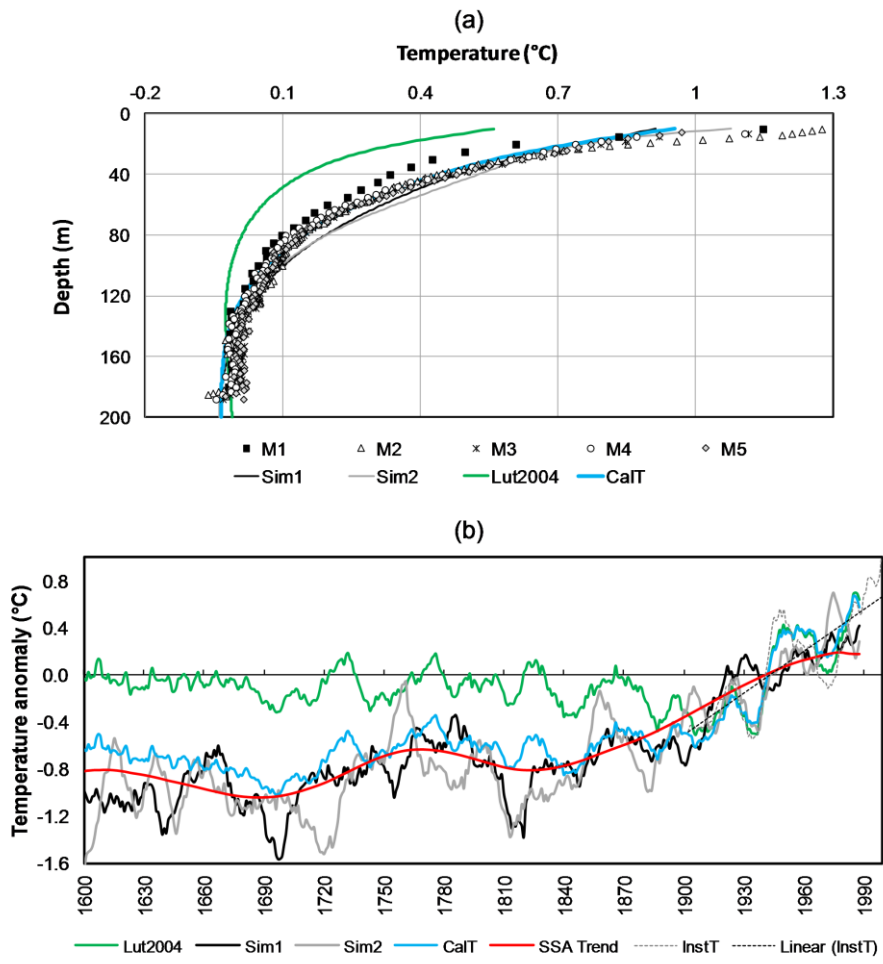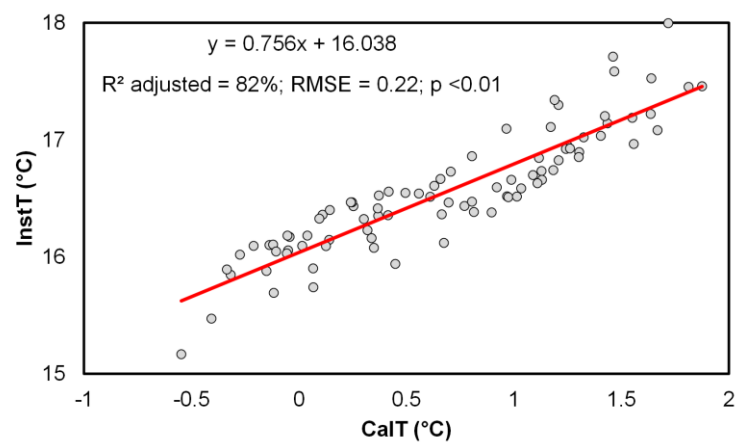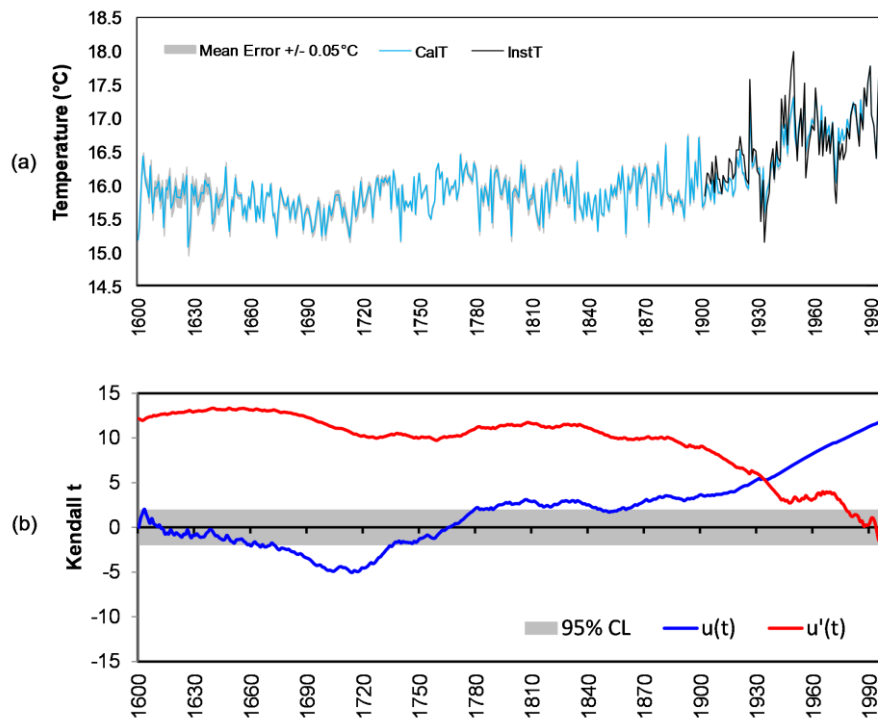
(a)

(b)

y_{M1} = 47.2x - 791.9 (RMSE=0.005ºC)
y_{M2} = 46.0x - 767.7 (RMSE=0.009ºC)
y_{M3} = 47.7x - 800.4 (RMSE=0.007ºC)
y_{M4} = 48.0x - 808.0 (RMSE=0.008ºC)
y_{M5} = 48.1x - 809.0 (RMSE=0.008ºC)

■ M1 ▲ M2 ✕ M3 ● M4 ◆ M5

603
604
605

Fig. 1

21

(a)

Temperature (°C)

(b)

606
607
608

Fig. 2

22

y = 0.756x + 16.038

R² adjusted = 82%; RMSE = 0.22; p <0.01

609
610
611

Fig. 3

23

Fig. 4

612
613
614
615

616

617
618
619

Fig. 5

25